

Fluorescent pyrene-centered starburst oligocarbazoles with excellent thermal and electrochemical stabilities†

Ming-Guang Ren,^a Hui-Jun Guo,^b Fei Qi^b and Qin-Hua Song^{*a}

Received 30th May 2011, Accepted 30th June 2011

DOI: 10.1039/c1ob05857f

A series of pyrene-centered starburst oligocarbazoles (1–3) have been synthesized and well characterized. Based on photophysical, thermal and electrochemical studies in solutions and as thin films, all starburst molecules reveal a sky blue emission with a high efficiency ($\Phi_F = 0.99 - 0.81$) and excellent thermal and electrochemical stabilities. As OLED materials, these superior properties are helpful to enhance device stability and lifetime.

Introduction

In the past two decades, small organic molecules and conjugated polymers have received the most attention as new materials with a high efficiency and a long lifetime in the field of organic light-emitting diodes (OLED).¹ Besides small organic molecules and polymers, a new class of OLED materials, including dendrimers, starbursts and oligomers, has recently attracted great attention.² These macromolecules combine the merits of well-defined structures and superior chemical purity possessed by small molecules and simple solution-processing advantage of polymers.³ The well designed and controlled synthesis of molecules can offer desired properties, and have been widely used in a variety of applications from material to biology science.⁴

Recently, a few 1,3,6,8-substituted pyrene-centered starbursts and dendrimers were synthesized as OLED materials, including starburst oligofluorenes,^{5a} the fluorene-substituted carbazole end-capped starbursts,^{5b} and dendrimers with polyethylene shell,⁶ or fluorene/carbazole dendrons and acetylene as linkages.⁷ Above studies^{5–7} and reports on 1,3,6,8-tetrasubstituted pyrenes⁸ showed that pyrene-centered starbursts and dendrimers combine efficient photon-harvesting strong fluorescence, good thermal stability, good solubility and excellent film-forming properties. Especially, the introduction of carbazole unit can enhance the hole-injection capability of the materials, and improve thermal stability and

electrochemical stability.^{5b} A series of new carbazole dendrimers were synthesized by modified at 3-, 6-, and 9- positions, possessing a rigid and highly twisted structure, and producing a potential gradient of electron density.⁹ The special properties of oligocarbazole prompt us to explore the synthesis of pyrene-centered starburst oligocarbazoles.

In this work, we have synthesized three pyrene-centered starbursts oligocarbazoles (1–3, shown in Chart 1) and fully characterized them. These starbursts show superior properties including high fluorescence quantum efficiency, excellent thermal and electrochemical stabilities, which make them possible candidates for a class of solution processable blue emitters/hole injection in OLEDs.

Results and discussion

The synthesis procedures of starburst molecules 1–3 contain two parts: synthesis of the arm, carbazole/oligocarbazole boronic acids (Scheme 1) and synthesis of starburst molecules by a Suzuki cross-coupling between 1,3,6,8-tetrabromopyrene and the corresponding boronic acids (Scheme 2). First, bromination of carbazole with NBS in different proportions at room temperature has provided compounds **4**¹⁰ and **7**,¹¹ respectively. Second, *N*-alkylation of **4**, **7** and carbazole with 1-octylbromide have been carried out at 120 °C in toluene and 50% NaOH solution containing tetra-*n*-butylammonium bromide (TBAB) as a phase-transfer catalyst, giving **5**,¹⁰ **8**¹¹ and **9**^{8b} in quantitative yields, respectively. Transformation of the bromide **5** into corresponding boronic acid **6** has been performed by lithium-bromide exchange at low temperature, followed by reacted with trimethyl borate at low temperature, and subsequent acid hydrolysis at room temperature. Third, the palladium-catalyzed Suzuki cross-coupling of one equivalents of **6** with 2.5 eq of **8** and **11** affords **12** and **14**, respectively. **10**,^{8b} **11**^{8b} and 1,3,6,8-tetrabromopyrene (**16**)¹² has been prepared according to the literatures. Fourth, transformations of the bromides **12** and **14** into the corresponding boronic acid **13** and **15** are carried out by the same procedure with synthesis of **6**, respectively. At last, Suzuki cross-coupling reactions between **16** and excess of boronic acids **6**, **13**, **15** using Pd(PPh₃)₄ as a catalyst afforded the desired starburst molecules 1–3 in excellent yield, respectively (Scheme 2). The monodisperse starburst molecules were identified by ¹H and ¹³C NMR spectroscopy, MALDI-TOF MS and elemental analysis.

The absorption and photoluminescence of 1–3 were investigated both in solutions and as thin neat films. Fig. 1 shows the

^aDepartment of Chemistry, Joint Laboratory of Green Synthetic Chemistry, University of Science and Technology of China, Hefei, 230026, China. E-mail: qhsong@ustc.edu.cn; Fax: +86 551 3601592; Tel: +86 551 3607524

^bNational Synchrotron Radiation Laboratory, University of Science and Technology of China, Hefei, 230029, P.R. China

† Electronic supplementary information (ESI) available: Experimental details, calculation results and solvent effects on the absorption and fluorescence spectra, of 1–3, and characterization data of new compounds **6**, **12–15**, **1**, **2** and **3**; and copies of mass spectra of 1–3 and NMR spectra of new compounds. See DOI: 10.1039/c1ob05857f

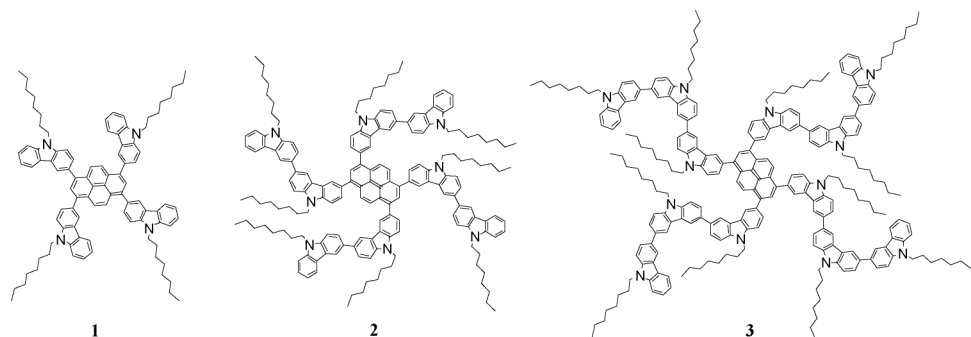
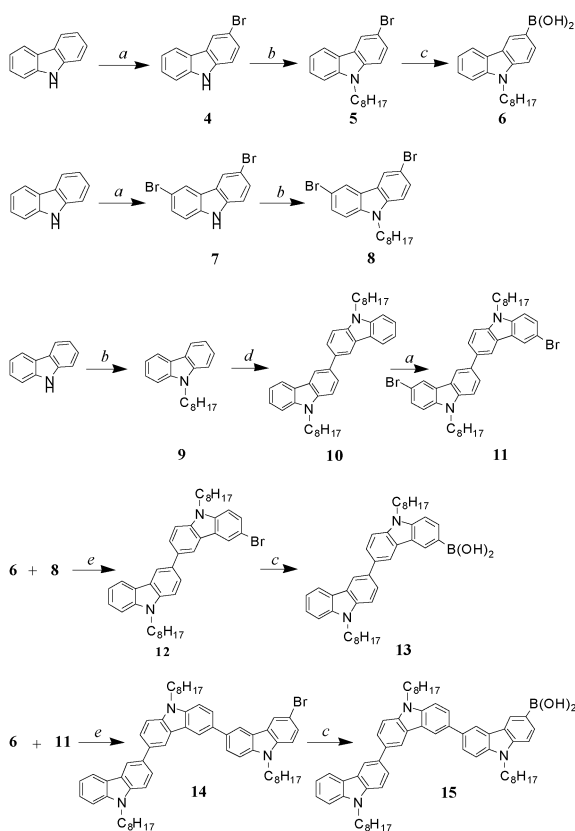
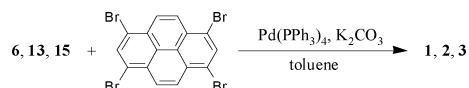


Chart 1 Structures of three pyrene-centered starburst oligocarbazoles.



Scheme 1 The synthetic routes of oligocarbazole boronic acids. Reagents and conditions: (a) NBS DMF r.t.; (b) Octylbromide, TBAB toluene, 50% NaOH reflux; (c) (i) *n*-BuLi, THF, -78°C ; (ii) $\text{B}(\text{OCH}_3)_3$, -78°C ; (iii) $\text{HCl}/\text{H}_2\text{O}$; (d) FeCl_3 , CHCl_3 ; (e) $\text{Pd}(\text{PPh}_3)_4$, K_2CO_3 , toluene.



Scheme 2 Synthesis of starburst molecules **1–3** by a Suzuki cross-coupling reaction.

absorption spectra and the fluorescence emission spectra of **1–3** in dichloromethane solutions. The absorption in a long-wavelength region should be assigned to the HOMO–LUMO transition of these molecules, and absorption peaks (λ_{max}) are 408, 410 and 402 nm for **1–3**, respectively. These peaks reflect the conjugation extent between the pyrene core and oligocarbazole arms. However, no uniform red-shift occurs when the arm length increases, and

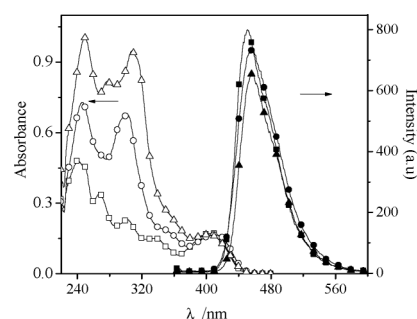


Fig. 1 Absorption spectra (open) ($2.5 \times 10^{-6}\text{M}$) and fluorescence emission spectra (full) of compounds **1** (square), **2** (circle) and **3** (triangle) in dichloromethane solutions, $\lambda_{\text{ex}} = 408\text{ nm}$.

λ_{max} first increases for **1** and **2** and then decreases for **3**. This may be due to steric inhibition of resonance between the pyrene core and the arms. The absorption band in the UV region is predominantly attributed to the carbazole or oligocarbazole arms, and molar extinction coefficients increases with the arm length, and data are listed in Table 1. For thin films, all absorption peaks have a bit red-shift relative to the solutions, that is, λ_{max} are 415, 416 and 407 nm for **1–3**, respectively. This may be a some extent of face-to-face stacking that leads to the aggregates formation of pyrene rings.

The fluorescence spectra of **1–3** in both dilute CH_2Cl_2 solutions and thin films display one emission peaks around 460 nm (solution) or 470 nm (film), with a narrow full width at half-emission maximum (fwhm) of 51–57 nm (solution) or 63–68 nm (film) (Fig. 1 and Fig. 2). Comparing to the solutions, the maximum emission peaks of the films have red-shift of 14 nm,

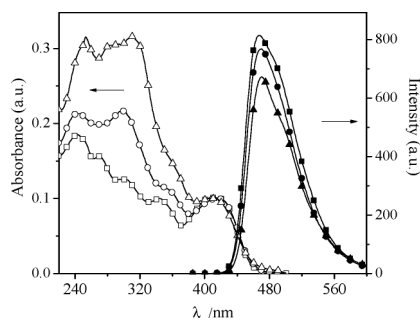


Fig. 2 Absorption spectra (open) and fluorescence emission spectra (full, $\lambda_{\text{ex}} = 408\text{ nm}$) of compounds **1** (square), **2** (circle) and **3** (triangle) as thin films prepared by spin-coating 5 wt% THF solutions of starbursts on glass substrate at a spin speed of 2000 rpm.

Table 1 Photophysical and electrochemical properties of starbursts 1–3

Compd.	$\lambda_{\text{abs}}/\text{nm}$		$\lambda_{\text{em}}/\text{nm}$		Φ_{F}^b	$E_{1/2}^c$ (V)	HOMO/LUMO (eV)	T_g/T_d /°C
	CH_2Cl_2	Film	CH_2Cl_2	Film				
1	240 (1.92 ^a), 267 (1.36), 302 (0.92), 338 (0.60), 408 (0.69)	243, 270, 304, 344, 415	454	468	0.99 (0.83)	1.13, 1.07	-5.57/-2.53	209/451
2	246 (2.92), 302 (2.69), 410 (0.66)	248, 304, 355, 416	461	470	0.91 (0.78)	1.05	-5.55/-2.52	264/459
3	249 (4.01), 277 (3.13), 308 (3.78), 402 (0.67)	252, 280, 310, 407	460	470	0.81 (0.72)	0.95	-5.45/-2.36	307/463

^a The values in brackets are molar extinction coefficient, $10^5 \text{ M}^{-1} \text{ cm}^{-1}$. ^b $\lambda_{\text{ex}} = 408 \text{ nm}$ ($\lambda_{\text{ex}} = 300 \text{ nm}$). ^c Half-wave oxidation potentials vs. Fc^+/Fc , a glassy carbon working electrode, $0.1 \text{ M Bu}_4\text{NPF}_6\text{-CH}_2\text{Cl}_2$, scan rate 100 mV s^{-1} .

9 nm and 10 nm for 1–3, respectively, and the fwhms have 10 nm widened. Despite so, it did not lead to the appearance of low-energy emission bands resulting from the possible aggregating. Using fluorescein as a reference ($\Phi_{\text{F}} = 0.90^{13}$ in 0.1 N NaOH), the fluorescence quantum yields (Φ_{F}) of 1–3 in dichloromethane have been measured to be 0.99, 0.91 and 0.81, respectively, and decreases as the arm increases. The decrease in the quantum yield may be due to the increase in the nonradiative deactivation resulting from the un-rigid arms.

When the starbursts are excited in the absorption range of 300–390 nm, the emission spectra for all three molecules only show one emission peak from the core. The single emission upon excitation of carbazole arms suggests the occurrence of efficient intramolecular energy transfer (Fig. 3). The quantum efficiency decreases with excitation wavelength, largely decreasing when the excitation wavelength is lower than 300 nm. Using quinine sulfate solution in $0.1 \text{ N H}_2\text{SO}_4$ ($\Phi_{\text{F}} = 0.546^{14}$) as a reference, fluorescence quantum yields obtained under excitation at 300 nm are lower than those of excitation at 408 nm (Table 1). The quantum efficiency decreases as the arm length increases. A similar observation was obtained from conjugated dendrimers with a pyrene core, fluorene/carbazole dendrons.^{7a}

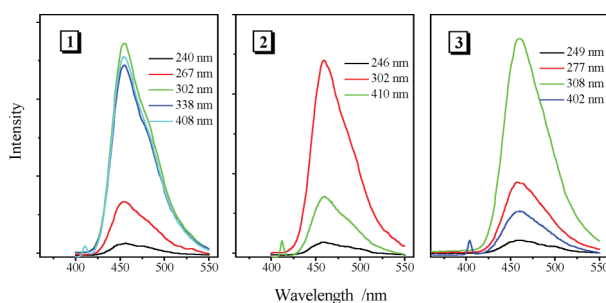


Fig. 3 Fluorescence spectra of 1–3 in dichloromethane solutions at different excitation wavelength.

The electrochemical behavior of 1–3 has been examined by CV using a standard three-electrode cell in an electrolyte solution 0.1 M tetrabutylammonium hexafluorophosphate [TBAPF_6] dissolved in dichloromethane. The working electrode is glassy carbon, the counterelectrode is a platinum wire, and the reference electrode is saturated calomel electrode (SCE). The CV voltammograms are shown in Fig. 4, using ferrocene as a standard.¹⁵ There are two oxidation peaks for 1, only one for 2 and 3, which are well-defined reversible redox waves for each starburst. Fig. 4

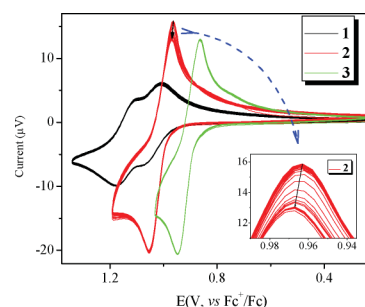


Fig. 4 Cyclic voltammograms of the starbursts 1–3 in CH_2Cl_2 solutions.

exhibits only a very small shift to higher voltage after 25 scan cycles for 1 and 3, 50 cycles for 2 ($<4 \text{ mV}$). This shows that these starbursts have excellent electrochemical stability, and can withstand more times a redox cycle than the carbazole end-capped pyrene starburst giving a 100 mV shift to higher voltage after 8 scan cycles.^{5b} This electrochemical stability is unprecedented.^{5,7a,8d} Thus, as OLED materials, these starbursts would enhance their service time in device operation. The values of the half-wave oxidation potentials ($E_{1/2}$) for 1–3 are 1.07 V , 1.05 V and 0.95 V , respectively. Obviously, the oxidation potential decreases with increasing the arm length. Quantum chemical calculation shows that from 1 to 3 the HOMO becomes located on the carbazole arms and the LUMO on the pyrene (see details in ESI†). Solvent effects on fluorescence spectra of 1–3 support this calculated result. From 1 to 3, the solvatochromic effect on fluorescence emission becomes notable, implying an intramolecular charge transfer process from the arm to the pyrene core occurs (see Table S2 in ESI†). This implies that although the conjugation between the pyrene core and arms first increases and then decreases, the carbazole arm reveals a uniform increase of conjugation. On the basis of the half-wave oxidation potentials, the highest occupied molecular orbital (HOMO) energy levels of starbursts are estimated in the range of -5.57 to -5.45 ($\text{HOMO} = E_{1/2} + 4.5 \text{ eV}^{16}$). The lowest unoccupied molecular orbital (LUMO) energy level are ranged from -2.36 to -2.53 eV , calculated from the HOMO energy level and energy band gap (E_g , eV) based on their fluorescence spectra ($\text{LUMO} = \text{HOMO} + E_g$). The data suggest that starbursts molecules with higher generation possess higher energy levels.

The thermal stability of the starbursts is examined by differential scanning calorimetry (DSC) and thermogravimetric analysis (TGA) in N_2 at a heating rate $10 \text{ }^\circ\text{C}$, shown in Fig. 5. All compounds exhibit very high glass transition temperature (T_g) and decomposition temperature (T_d), at which 5% of mass

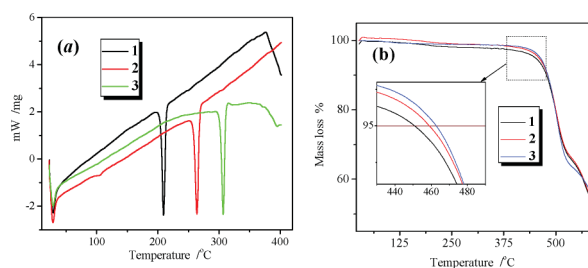


Fig. 5 (a) DSC thermograms of 1–3 and (b) TGA thermograms of 1–3 under a nitrogen atmosphere at a heating rate of $10\text{ }^{\circ}\text{C min}^{-1}$.

loss occurs, and data are listed in Table 1. Both T_g and T_d increase with the molecular size. The oligocabazole in 3,6-linking mode can significantly improve thermal properties of the pyrene-centered starbursts. Both T_g and T_d of starbursts 1–3 are much higher over those of pyrene-centered starburst oligofluorenes (T_g : $62\text{--}92\text{ }^{\circ}\text{C}$ and T_d : $378\text{--}391\text{ }^{\circ}\text{C}$),^{5a} the carbazole end-capped pyrene starburst (T_d : $299\text{ }^{\circ}\text{C}$),^{5b} and pyrene-centered dendrimers conjugated with fluorene/carbazole dendrans (T_g : $128\text{--}174\text{ }^{\circ}\text{C}$ and T_d : $425\text{--}442\text{ }^{\circ}\text{C}$).^{7a} This shows these compounds possess excellent thermal stability. The high thermal stability is advantage for OLED applications, which is helpful to enhance device stability and lifetime.

Conclusion and future work

We have synthesized three pyrene-centered starburst oligocabazoles via a 3,3' carbon-carbon coupling, and full characterized them with ^1H and ^{13}C NMR spectroscopy, MS and elemental analysis. These starbursts reveal only one emission peak with a high efficiency, and unprecedented electrochemical and thermal stabilities, which could greatly enhance their service time as OLED materials in device operation. Furthermore, we will investigate their electroluminescence and improve the device performance with these starbursts as the hole-injection/light-emitting layer.

Acknowledgements

This work was supported by the National Natural Science Foundation of China (Grant Nos. 30870581, 20972149) and the Graduate Innovation Fund of USTC.

Notes and references

1 B. W. D'Andrade and S. R. Forrest, *Adv. Mater.*, 2004, **16**, 1585; C. T. Chen, *Chem. Mater.*, 2004, **16**, 4389; P. I. Shih, Y. H. Tseng, F. I. Wu, A. K. Dixit and C. F. Shu, *Adv. Funct. Mater.*, 2006, **16**, 1582.

- 2 A. W. Freeman, S. C. Koene, P. R. L. Malenfant, M. E. Thompson and J. M. J. Fréchet, *J. Am. Chem. Soc.*, 2000, **122**, 12385; P. Furuta, J. Brooks, M. E. Thompson and J. M. J. Fréchet, *J. Am. Chem. Soc.*, 2003, **125**, 13165; T. W. Kwon, M. M. Alam and S. A. Jenekhe, *Chem. Mater.*, 2004, **16**, 4657; W. E. Howard, *Sci. Am.*, 2004, **290**, 64; T. D. Anthopoulos, M. J. Frampton, E. B. Namdas, P. L. Burn and I. D. W. Samuel, *Adv. Mater.*, 2004, **16**, 557; E. Holder, B. M. W. Langeveld and U. S. Schubert, *Adv. Mater.*, 2005, **17**, 1109; P. L. Burn, S. C. Lo and I. D. W. Samuel, *Adv. Mater.*, 2007, **19**, 1675; D. H. Choi, K. I. Han, I. H. Chang, S. H. Choi, X. H. Zhang, K. H. Ahn, Y. K. Lee and J. Jang, *Synth. Met.*, 2007, **157**, 332; H. J. Bolink, E. Barea, R. D. Costa, E. Coronado, S. Sudhakar, C. Zhen and A. Sellinger, *Org. Electron.*, 2008, **9**, 155.
- 3 (a) J. N. G. Pillow, M. Halim, J. M. Lupton, P. L. Burn and I. D. W. Samuel, *Macromolecules*, 1999, **32**, 5985; (b) J. M. Lupton, I. D. W. Samuel, R. Beavington, P. L. Burn and H. Bässler, *Adv. Mater.*, 2001, **13**, 258; (c) M. J. Frampton, R. Beavington, J. M. Lupton, I. D. W. Samuel and P. L. Burn, *Synth. Met.*, 2001, **121**, 1671; (d) D. G. Ma, Y. F. Hu, Y. G. Zhang, L. X. Wang, X. B. Jing, F. S. Wang, J. M. Lupton, I. D. W. Samuel, S. C. Lo and P. L. Burn, *Synth. Met.*, 2003, **137**, 1125.
- 4 G. R. Newkome, C. N. Moorefield and F. Vögtle, *Dendrimers and Dendrons*, Wiley-VCH: Weinheim, Germany, 2001; J. M. J. Fréchet and D. A. Tomalia, ed. *Dendrimers and Other Dendritic Polymers* Wiley-VCH: Chichester, UK, 2001; D. A. Tomalia and J. M. J. Fréchet, *Prog. Polym. Sci.* 2005, **30**, 217; J. P. Majoral, *New J. Chem.*, 2007, **31**, 1039.
- 5 (a) F. Liu, W. Y. Lai, C. Tang, H. B. Wu, Q. Q. Chen, B. Peng, W. Wei, W. Huang and Y. Cao, *Macromol. Rapid Commun.*, 2008, **29**, 659; (b) F. Liu, J. H. Zou, Q. Y. He, C. Tang, L. H. Xie, B. Peng, W. Wei, Y. Cao and W. Huang, *J. Polym. Sci., Part A: Polym. Chem.*, 2010, **48**, 4943.
- 6 S. Bernhardt, M. Kastler, V. Enkelmann, M. Baumgarten and K. Müllen, *Chem.–Eur. J.*, 2006, **12**, 6117; T. Qin, W. Wiedemair, S. Nau, R. Trattnig, S. Sax, S. Winkler, A. Vollmer, N. Koch, M. Baumgarten, E. J. W. List and K. Müllen, *J. Am. Chem. Soc.*, 2011, **133**, 1301.
- 7 (a) Z. J. Zhao, J. H. Li, X. P. Chen, X. M. Wang, P. Lu and Y. Yang, *J. Org. Chem.*, 2009, **74**, 383; (b) Y. Wan, L. Y. Yan, Z. J. Zhao, X. N. Ma, Q. J. Guo, M. L. Jia, P. Lu, G. Ramos-Ortiz, J. L. Maldonado, M. Rodriguez and A. D. Xia, *J. Phys. Chem. B*, 2010, **114**, 11737.
- 8 (a) V. de Halleux, J. P. Calbert, P. Brocorens, J. Cornil, J. P. Drclercq, J. L. Brédas and Y. Geevts, *Adv. Funct. Mater.*, 2004, **14**, 649; (b) G. Venkataraman and S. Sankaraman, *Eur. J. Org. Chem.*, 2005, 4162; (c) Y. H. Park, H. H. Rho, N. G. Park and Y. S. Kim, *Curr. Appl. Phys.*, 2006, **6**, 691; (d) P. Sonar, M. S. Soh, Y. H. Cheng, J. T. Henssler and A. Sellinger, *Org. Lett.*, 2010, **12**, 3292.
- 9 K. Albrecht and K. Yamamoto, *J. Am. Chem. Soc.*, 2009, **131**, 2244.
- 10 W. Huang, S. J. Ji, G. L. Feng and W. Y. Lai, *Synlett*, 2006, 2841.
- 11 Y. Li, J. Ding, M. Day, Y. Tao, J. Lu and M. D'Iorio, *Chem. Mater.*, 2004, **16**, 2165.
- 12 K. Brunner, A. van Dijken, H. Börner, J. J. A. M. Bastiaansen, N. M. M. Kiggen and B. M. W. Langeveld, *J. Am. Chem. Soc.*, 2004, **126**, 6035.
- 13 W. R. Dawson and M. W. Windsor, *J. Phys. Chem.*, 1968, **72**, 3251.
- 14 J. N. Demas and J. A. Crosby, *J. Phys. Chem.*, 1971, **75**, 991.
- 15 N. G. Connelly and W. E. Geiger, *Chem. Rev.*, 1996, **96**, 877.
- 16 T. Johansson, W. Mammo, M. Svensson, M. R. Andersson and O. Inganäs, *J. Mater. Chem.*, 2003, **13**, 1316.